

UNCLASSIFIED

AD 274 161

*Reproduced
by the*

**ARMED SERVICES TECHNICAL INFORMATION AGENCY
ARLINGTON HALL STATION
ARLINGTON 12, VIRGINIA**



UNCLASSIFIED

NOTICE: When government or other drawings, specifications or other data are used for any purpose other than in connection with a definitely related government procurement operation, the U. S. Government thereby incurs no responsibility, nor any obligation whatsoever; and the fact that the Government may have formulated, furnished, or in any way supplied the said drawings, specifications, or other data is not to be regarded by implication or otherwise as in any manner licensing the holder or any other person or corporation, or conveying any rights or permission to manufacture, use or sell any patented invention that may in any way be related thereto.

274161

FILE COPY

**Return to
ASTIA**

**ARLINGTON HALL STATION
ARLINGTON 12, VIRGINIA**

Attn: TIRS

SPACECRAFT THERMODYNAMICS SYMPOSIUM

28 MARCH 1962

**LMSC RESEARCH LABORATORIES
PALO ALTO, CALIFORNIA**



Discoverer Orbital Thermodynamic Design-Predictions and Flight Data Correlation

N. Cahan and E. A. LaBlanc
Lockheed Missiles & Space Company

Methods used for predicting space vehicle structural and equipment temperatures on orbit are presented. The energy balance between the vehicle, deep space, the sun, and the earth is applied to determine dynamic temperature histories for vehicle equipment. Data received from vehicles on orbit are compared to predictions. Certain anomalies are investigated and their causes determined. Application of flight results to vehicle design and prediction methods is described.



The successes and failures of the 35 Discoverer vehicles which have been flown have provided an excellent opportunity and a challenge in the prediction of orbital thermal performance of a space vehicle. The analyses of data obtained from flight have shown that accurate orbital predictions are still as much an art as a science, and that large errors in predictions may result from small and apparently (at the time) minor errors in input data.

In general, however, the techniques used in analyzing theoretical Discoverer thermodynamic performance have been shown by flight results to be reliable and capable of producing predictions useful as bases for spacecraft and equipment design.

METHOD OF ANALYSIS

Consider an isolated homogeneous body orbiting the earth at moderate altitude. The energy balance between the body and its environment when in dynamic equilibrium includes the following energy inputs (Ref. 1):

- Solar radiation**
- Albedo radiation (energy reflected by earth and its atmosphere)**
- Earthshine (energy emitted by earth)**
- Internal energy dissipation (such as electrical power)**

All this energy must be dissipated to space by radiation. The steady-state energy balance may be written, on a unit area basis,

$$q = \sigma\epsilon T_a^4 = \alpha_S F_S S + \alpha_E F_E E + \alpha_R F_R R + P_i \quad (1)$$

where T_a is the average temperature of the body.

It may be shown that, for engineering purposes,

$$\alpha_S = \alpha_R$$

and

$$\alpha_E = \epsilon$$

The average temperature of the body is then

$$T_a = \left\{ \sigma \left[\frac{\alpha_S}{\epsilon} (F_S S + F_R R) + F_E E + \frac{P_i}{\epsilon} \right] \right\}^{1/4} \quad (2)$$

It is seen that the temperature is a function of the ratio α_S/ϵ as well as the absolute value of the emissivity. The relative importance of the two terms depends upon the quantity of internal energy P_i being dissipated.

A family of plots of the time average temperature of a homogeneous vertical cylinder orbiting at 300 mi as a function of the ratio α_S/ϵ is given in Fig. 1. Curves are given for three values of the solar incidence angle β . The approximate values of α_S/ϵ for a number of surface finishes are plotted. The temperature ranges shown here are averages in time (for $\beta = 90$ deg) and apply to a homogeneous body with no appreciable temperature gradients. A portion of a body in which gradients can exist will have higher temperatures when on the sunward side and lower when on the dark side.

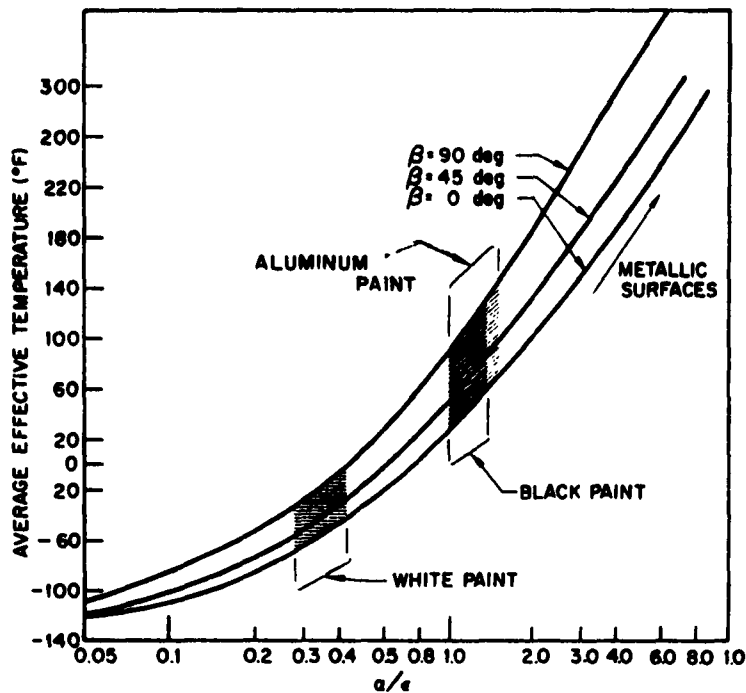


Fig. 1 Time Average Temperature of a Homogeneous Vertical Cylinder Orbiting at 300 Mi

Real satellites are not homogeneous bodies, but are composed of skin and structure, have various pieces of equipment mounted on and in them, and may be in a steady-state heat balance or a transient (steady-state dynamic) condition, influenced by the duty cycles of vehicle equipment and payload as well as cyclic patterns of solar heating as the vehicle moves into and out of the sunlight.

A definitive analysis of real satellite temperatures is feasible if the body in question can be visualized divided into many relatively small elements for solution by finite difference techniques. Each discrete element or node must be small enough to be considered isothermal. Experience has shown that a node can be as much as a complete piece of electronic gear, or a skin section no larger than approximately 16 in. by 16 in. This simplification encompasses about 85% of the electronic packages in

the Agena equipment racks, and allows realistic consideration of the internal power dissipation of each component. The skin sections cannot be chosen larger because the external heat rates must be considered uniform over the surface and equal to the rate at the nodal geometric center.

The instantaneous heat balance on any node (exposed to space) may now be expressed

$$\frac{dT}{dt} = \frac{1}{C} \left\{ \left[\sigma \epsilon T^4 + \sum \frac{\Delta T}{r_n} - P_i - \left[\alpha_s (F_s S + F_r R) + \epsilon F_e E \right] \right] \right\} \quad (3)$$

where $C = mc_p$ for the node. The term $\sum \frac{\Delta T}{r_n}$ represents the sum of all the instantaneous conduction and radiation heat-transfer paths between the node under consideration and all its neighbors.

The terms $F_s S$ and $F_r R$ are functions of time and must be calculated separately for the orbital geometry and location of the individual node on the satellite. Several graphical solutions have been prepared (Refs. 2 and 3) from which numerical values may be obtained for any geometry. More recently, a digital computer routine has been developed which provides instantaneous heat rates in response to inputs for a specific body shape in a particular earth orbit.

The net internal conduction is given by:

$$q_{ic} = \sum_n [K_1 (T_1 - T_N) + K_2 (T_2 - T_N) \dots K_n (T_n - T_N)] \quad (4)$$

where K is the conductance of adjacent nodes. Internal radiation energy transfer may be shown as:

$$q_{ir} = \sigma \sum_n [I_{1N} (T_1^4 - T_N^4) + I_{2N} (T_2^4 - T_N^4) \dots I_{nN} (T_n^4 - T_N^4)] \quad (5)$$

where \mathcal{J} is the radiation shape factor that includes the geometric area view factor between nodes and the appropriate effective emissivity of the net heat-transfer mechanism.

The internal power generation term P_i must be determined for each discrete segment according to its boundaries. It can be assumed that all electronic component power will be dissipated as thermal energy; the portion radiated as r-f energy is negligible.

Computation of Heat-Balance Differential Equation

High-speed digital programs have been set up for the solution of transient temperature histories for asymmetrical, three-dimensional networks defined by the preceding equations. These programs have assumed the name Thermal Network Analyzer because of their method of problem visualization and input. They are n-dimensional asymmetrical finite difference networks in which all the thermal parameters are entered into the computer in terms of their analogous electrical circuit counterparts.

These programs may be used for transient-temperature determination of any discrete part of a missile or satellite structure when simultaneously under the influence of aerodynamic heating; radiant energy interchange with solar, terrestrial, space, and secondary vehicle sources; conduction energy exchange with adjacent nodes; and internal heat generation. Aerodynamic heating will not be considered here because it is a low-order effect at these altitudes.

The thermal network of a space vehicle may be typified by the system shown in Fig. 2. The basic elements of thermal capacity, heat-transfer paths, and the external radiating surface are shown as well as the analogous electrical circuit. The total vehicle can be represented by many such systems, all interconnected to form a single unified network. The final representation is shown in Figs. 3 through 5, which represent the equipment bay in an early Agena vehicle. The numbers in these illustrations identify discrete equipment items or "lumped nodes" representative of portions of the structure and the interconnecting resistances. Each node has an associated value of thermal capacity and many include a time-dependent electrical power dissipation.

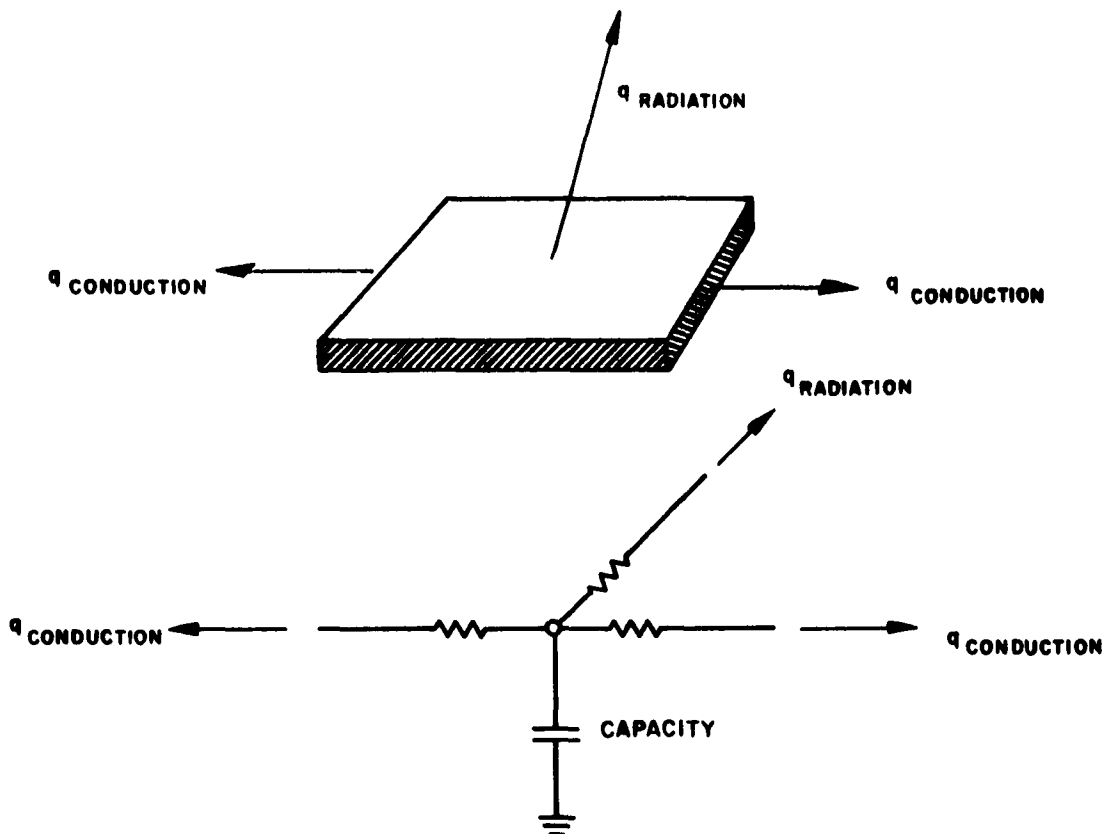


Fig. 2 Surface Node

The network to describe a section or bay of one vehicle, or a complete payload, may consist of hundreds of nodes.

Solutions to the extremely cumbersome equations describing these networks can be obtained quickly through the use of automatic digital computing machines utilizing the thermal analyzer program previously mentioned.

A typical node analogy is shown in Fig. 6. One end of each capacitor is always grounded. The number of connecting resistors among nodes is arbitrary. There is no required relationship between the node number and resistance numbers. The capacitances and heat inputs are referenced by the number of the node to which they are related. The transient solution for T_1 is found by relaxation of this network in

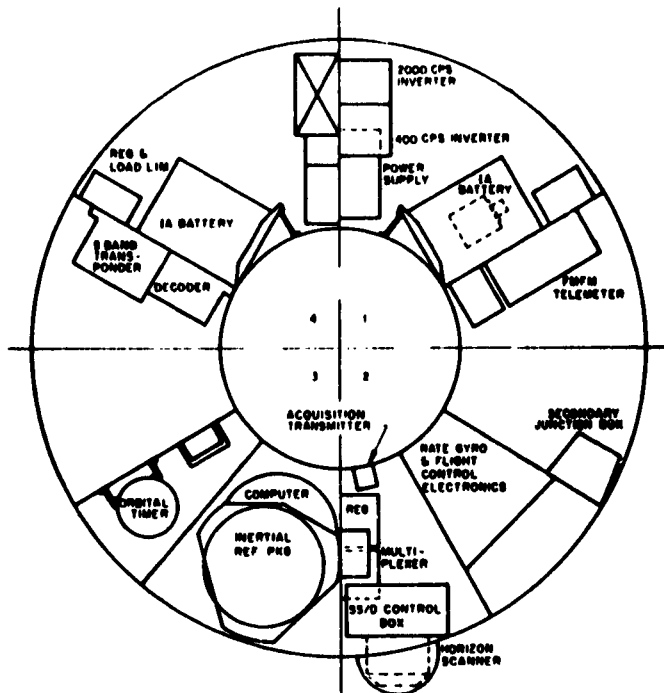


Fig. 3 Discoverer Equipment Bay

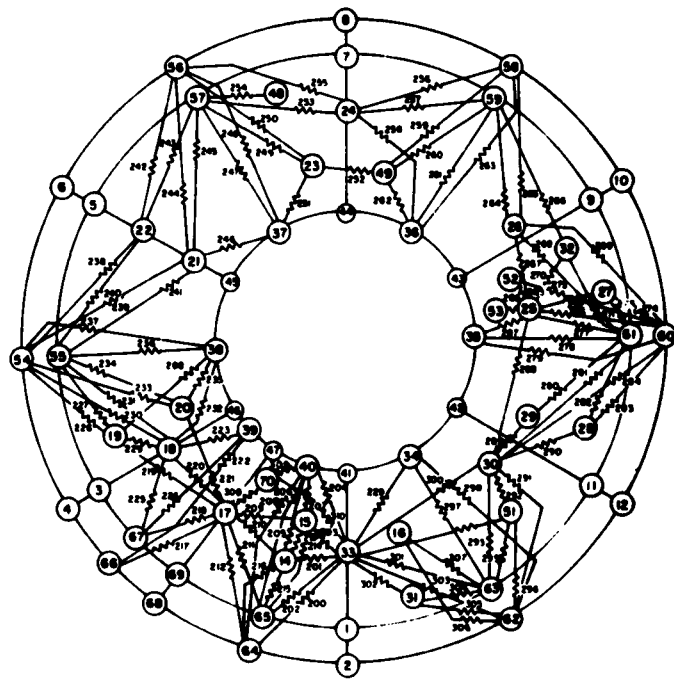


Fig. 4 Radiation Resistors for Discoverer Equipment Bay

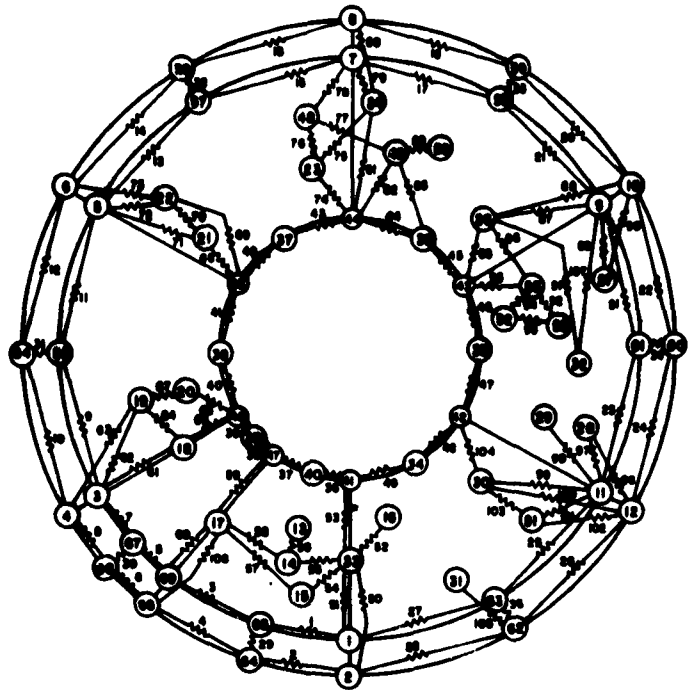


Fig. 5 Conduction Resistors for Discoverer Equipment Bay

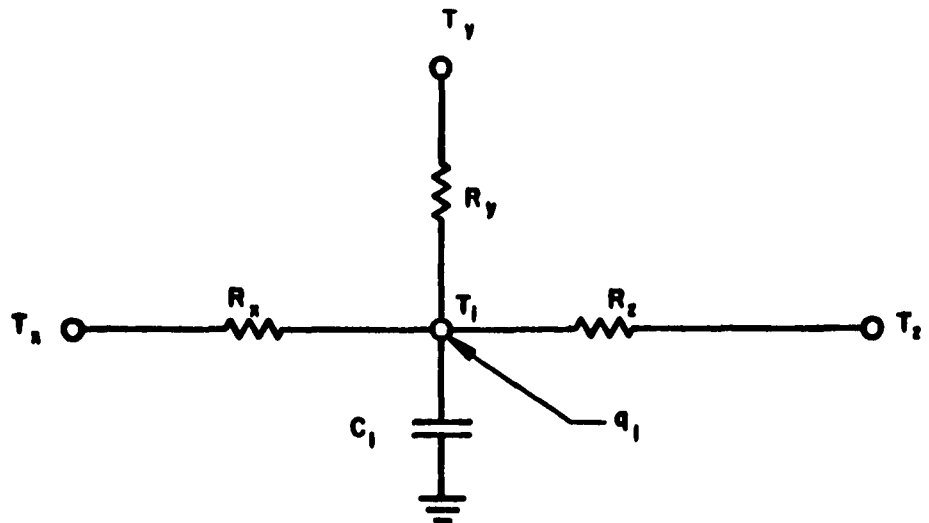


Fig. 6 Typical Network Node

time, assuming that all the remaining parameters are constant over the computing interval Δt . With this assumption, the differential equation representing the circuit shown in Fig. 2 is

$$\frac{dT_i}{dt} = \frac{1}{C_i} \left[q_i + \sum_{n=1}^N \frac{T_n}{r} - \sum_{n=1}^N \frac{T_n}{r} \right] \quad (5)$$

A very convenient form of solution for this linear, first-order differential equation, in terms of machine time and accuracy, is the following finite difference solution:

$$T_{i,t+\Delta t} = \frac{\Delta t}{C_i} \left(\sum_{n=1}^N \frac{T_{n,t}}{r_{i,n,t}} + q_i - T_{i,t} \sum_{n=1}^N \frac{T_n}{r} \right) + T_{i,t} \quad (6)$$

where

$T_{i,t+\Delta t}$ = the temperature of node i at time $t + \Delta t$

$T_{i,t}$ = the temperature of node i at time t

Δt = time increment (sec)

C_i = the thermal capacity of node i

$\sum_{n=1}^N$ = summation of all nodes connected to i by a resistor

$r_{i,n}$ = resistance between node i and any connected node N

q_i = the heat flowing into node i from sources other than environment – usually electrical energy

The time interval used to advance the transient solution is related to the physical parameters of the network. In particular, Δt must not exceed the minimum rC product for the network as this will result in instability in the solution of Eq. (6), causing undamped oscillation of temperatures for those nodes whose rC product is smaller than Δt .

Techniques Used in Employing the Thermal Network Analyzer

To facilitate handling the energy exchange between the vehicle and the earth, a simplifying method is used. As all bodies have emissive power of $\sigma\epsilon T^4$, all external energy sources may be visualized independently. The vehicle is thus assigned energy inputs from earth with view factors from the node under consideration to earth as time functions without regard to satellite temperature. For purposes of heat loss to space, a view factor of unity is applied to the node. This procedure greatly simplifies machine calculation of the energy balance between the vehicle and earth.

In the lumped parameter method, the heat rate is considered constant over some finite area. To ensure that the heat rate at the center of the surface is a good approximation for the entire node, the body angles included should not be larger than 30 deg. If a node must be assigned a larger included angle for some reason, the node mean heat rate can be approximated by averaging the heat rates for the body angles covered.

The external heat rates, or the incident radiant intensity of the external energy sources for every body angle have been compiled (Ref. 3). Figure 7 is a typical family of solar and albedo curves for $\beta = 0$. The heat rate absorbed from each source may be obtained by multiplying the incident heat rates by the solar absorptivity α_S or the infrared emissivity ϵ (whichever is applicable) of the surface finish. The absorbed heat rate may then be placed in the table look-up or general equation section of the arbitrary functions. When a parametric surface finish analysis is conducted for thermal control purposes, a new equation or heat-rate table is required. To minimize program changes and possible errors, the thermal circuit of Fig. 8 is used to input the external radiation received by a surface.

In this circuit, each input heat rate is treated as a varying temperature potential operating on the skin node through a resistor. The value of the driving temperature is programmed as a function of time to take into account orbital position θ . The resistor value is determined by the absorptance or emittance of the surface finish. The heat-rate input is made independent of the node temperature by the device of multiplying

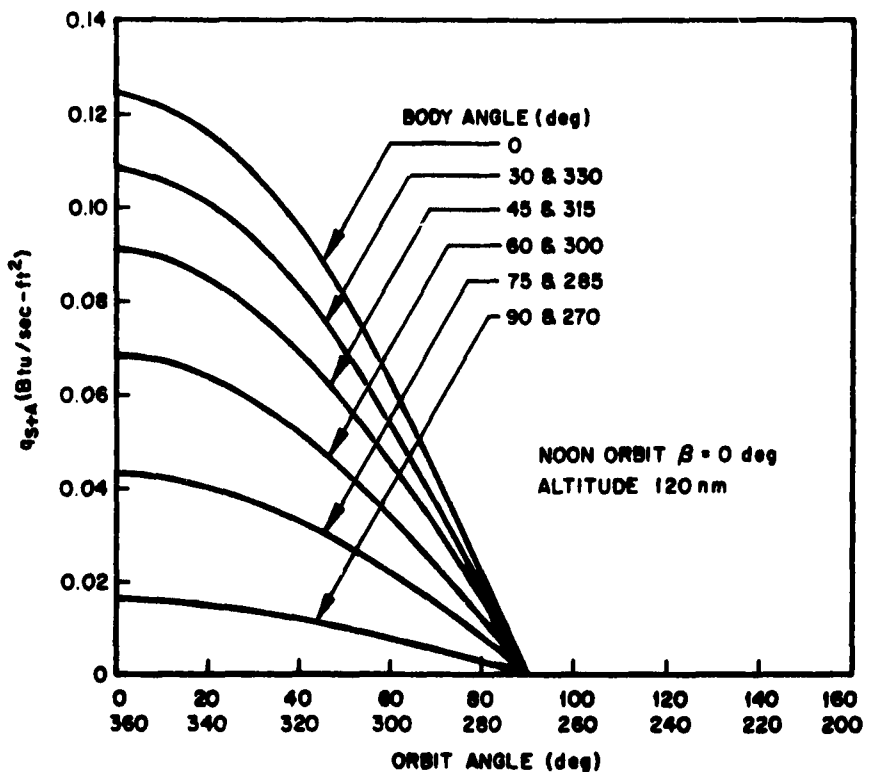


Fig. 7 Incident Solar and Albedo Radiation on a Horizontal Cylinder

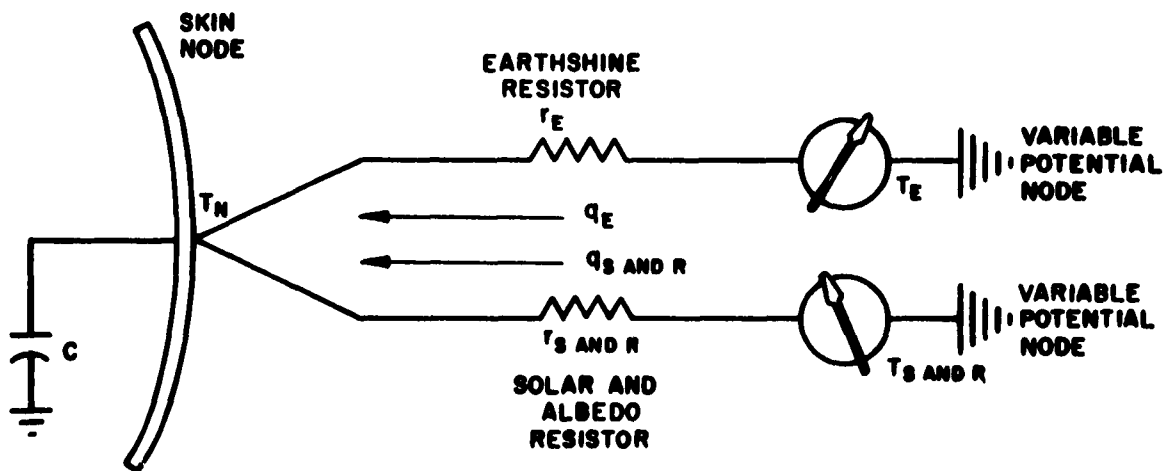


Fig. 8 Radiation Input Network

both driving temperature and resistor value by the same very large number, thus rendering the node temperature insignificant in determination of the heat rate.

This representation does not include the interrelated effects between vehicle nodes.

The end product of this analysis is design information rather than material of academic interest. Satellite equipment must be maintained within qualification temperature extremes for the duration of the mission.

An iterative procedure is therefore used in the planning of a new vehicle or major modification of an existing design. Preliminary layouts are made on the basis of previous experience and hand calculations of boundary conditions. These layouts are modified until a configuration is obtained which is apparently compatible with requirements.

While detailed design proceeds, the network representing the vehicle is built. Construction of the network is tied closely to the progress of the vehicle structural and equipment installation design. The completed network is solved on a trial basis, using a vehicle outer surface finish chosen as a first estimate. It is usual, at this point, to discover problems in equipment temperature. Solutions are proposed by means of internal structural modifications (insulators, conduction straps, relocation) and/or changes in outer surface finish, and the effects ascertained by reanalysis. Equation (2) demonstrates how local temperature may be controlled by choice of surface finishes to provide the requisite values of solar absorptance and infrared emittance. A large quantity of information is available to the analyst in Ref. 4, which contains the current results of a continuing laboratory surface spectral characteristic measurements program.

The resulting vehicle surface pattern may be one or more paints, in an arrangement by sectors and/or rings. A mosaic is used when the required characteristics are not available in a single paint or metallic surface. Figure 9 shows some typical patterns as used on Discoverer satellites. The choice of pattern is dictated by the anticipated orbital geometry.

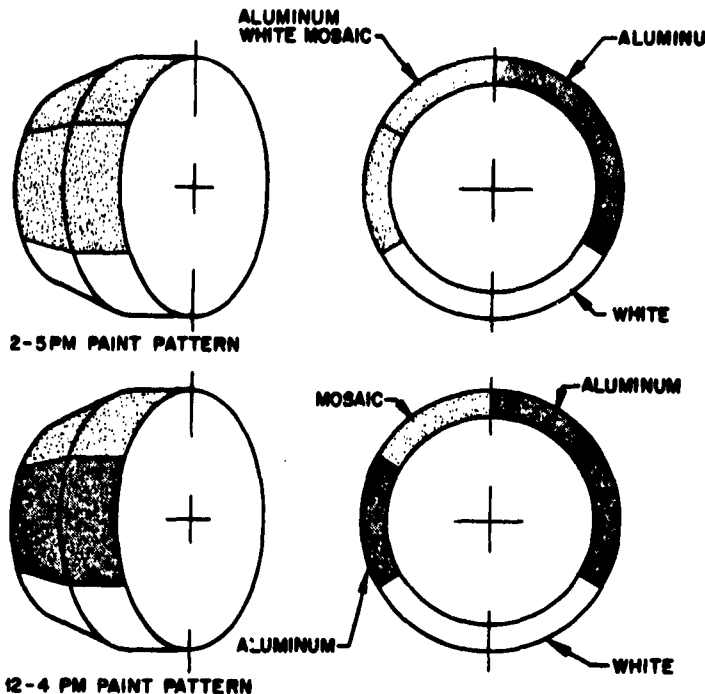


Fig. 9 Discoverer Forward Rack Paint Patterns

FLIGHT TEST RESULTS

Discoverer vehicles have carried temperature instrumentation on a number of pieces of equipment as well as on the vehicle skins. Unfortunately, several factors operate to detract from the usefulness of the data acquired. First, many of the measurements are "diagnostic"; that is, they are made to monitor the performance of specific pieces of equipment. Because of the limit on the number of telemetry channels available, these measurements frequently displace others of more interest to the analyst in confirming his predictions. Secondly, there has not been, to this date, a feasible method for acquiring data during an entire orbit; telemetry is obtained only as the vehicle passes over specific readout stations on the ground. These short bursts of data can never provide maximum temperatures, because of the location of the stations.

Figures 10 through 12 show data from a Discoverer flight, plotted on curves of the corresponding predictions. Although the agreement is good, there is no way to confirm the maximum values except indirectly by noting the temperature history of adjacent pieces of equipment of large thermal capacity, whose average temperature will be influenced by the time-average history of the skin node. The phase differences

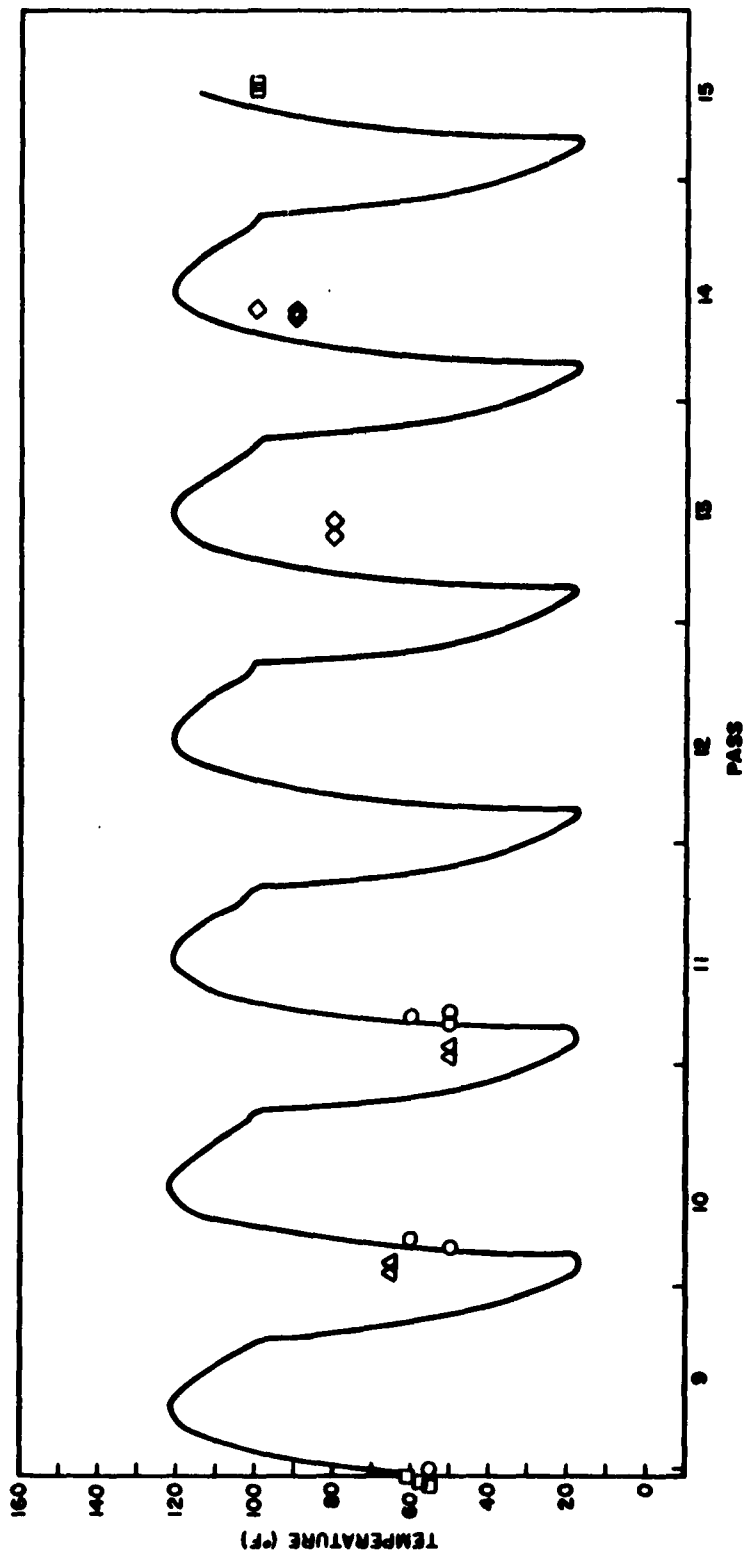


Fig. 10 Thermal Flight Data: Conical Skin Temperature

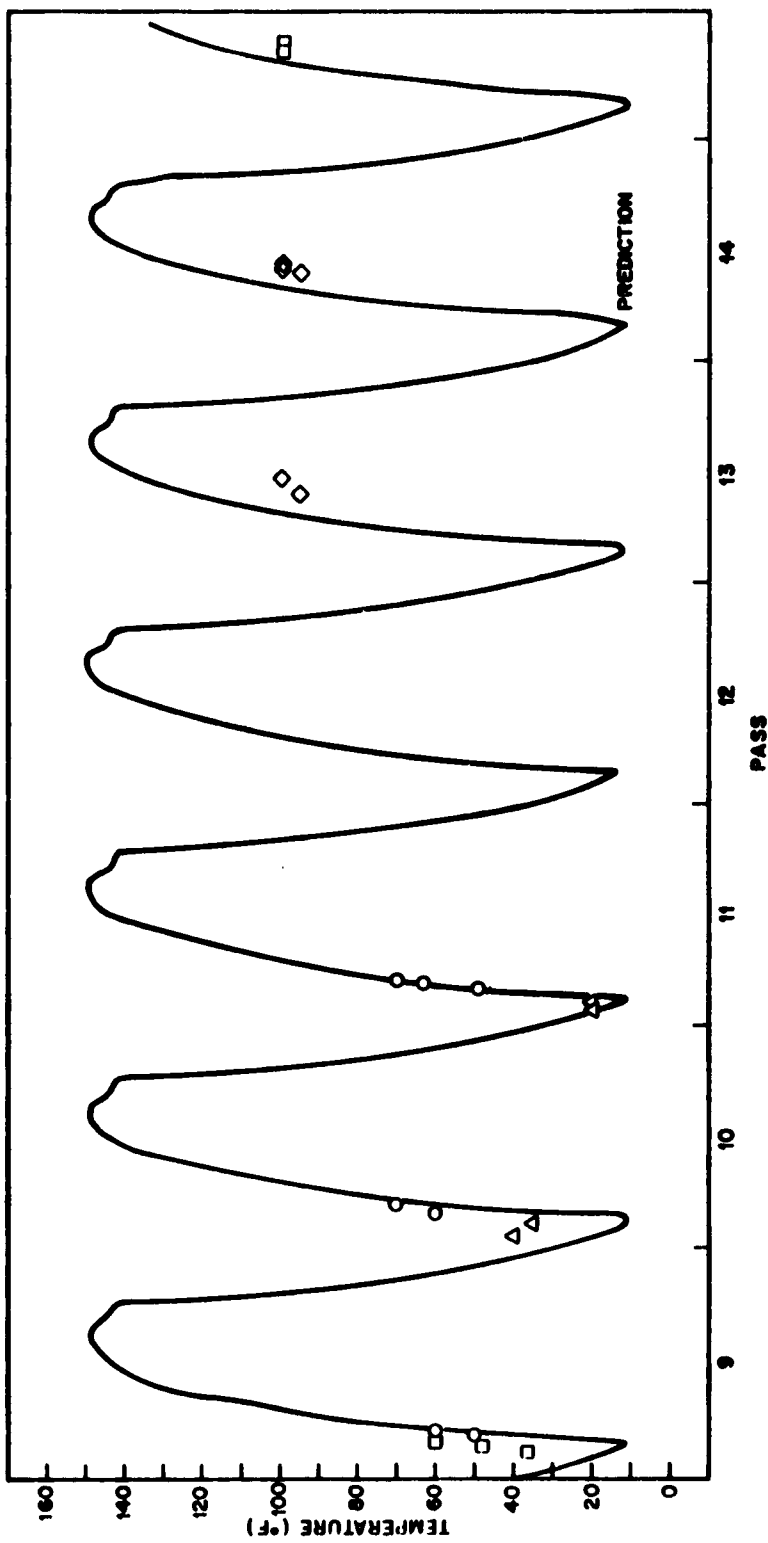


Fig. 11 Thermal Flight Data: Cylindrical Skin Temperature

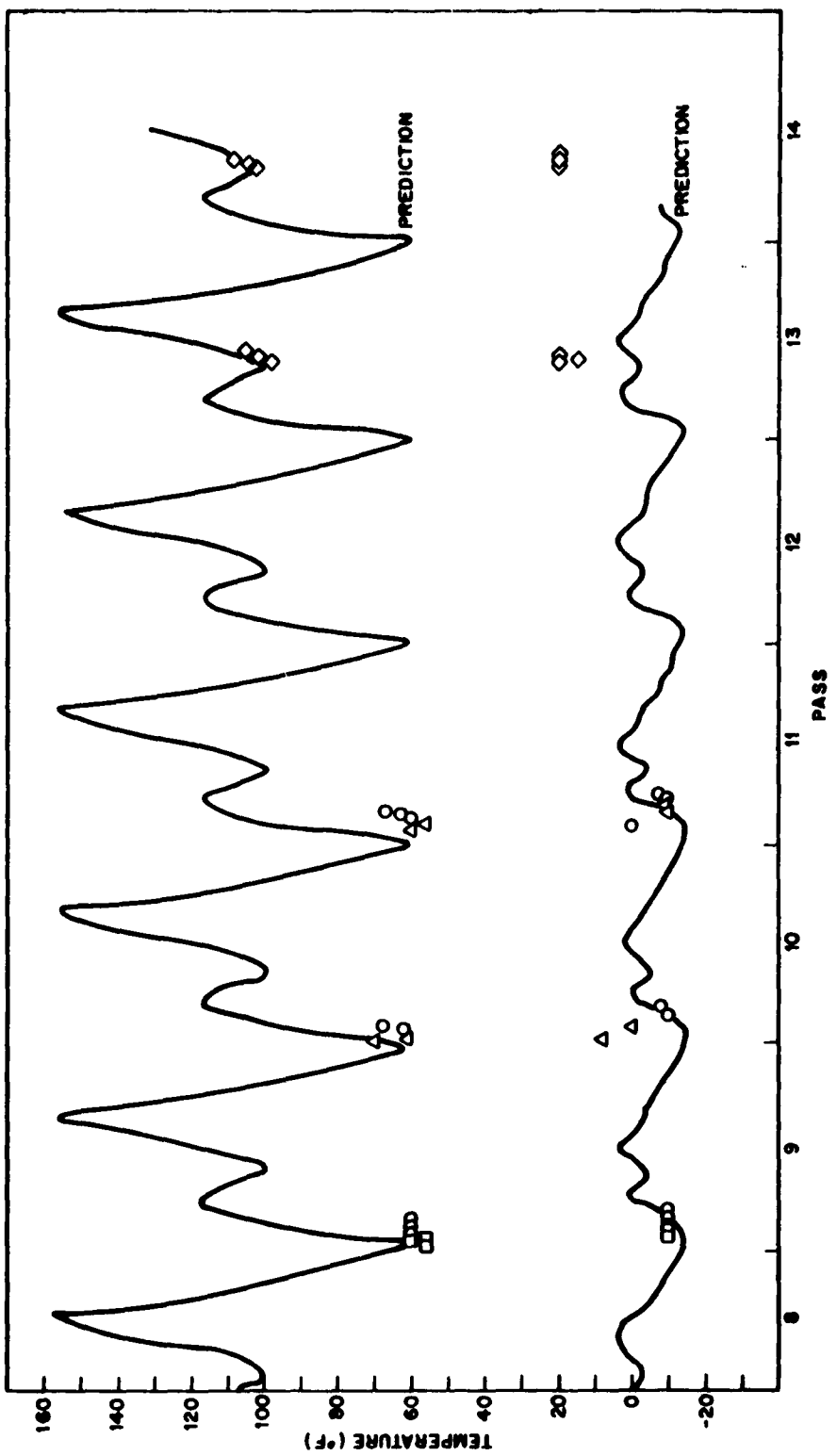


Fig. 12 Thermal Flight Data: Aft Equipment Rack Temperature

between the data and predictions are due to differences between the real orbit geometry and prediction; theoretical injection altitude and circularity cannot be achieved exactly.

The effect of an erroneous input of internal power dissipation, as well as a change in adjacent skin surface finish, is shown in Fig. 13. The original information gave an internal dissipation of 10 w for each primary battery. Because of the necessity to prevent overheating on orbits which would place that side of the vehicle in sunlight, white paint was used. The difference between prediction and data can be seen. A more intensive investigation revealed that dissipation averages 4 w in this service. Subsequently, it became desirable to operate the battery at a higher temperature. The sector was finished with an aluminum paint, and a new prediction made. The results are shown on the same figure.

Another phenomenon in battery behavior is shown in Fig. 14. It is seen that the battery temperature decays slowly after launch until, at about Pass 52, it begins to climb to a new level at which it stabilizes until Pass 84, when the useful flight is ending. It is hypothesized that this apparent anomaly is caused by the differences in potential between the several vehicle batteries, all tied in parallel to the common vehicle power bus. Early in the mission other batteries are carrying the load, resulting in a dissipation considerably lower than anticipated in the battery under study. When the other units have discharged enough to lower their available terminal voltage, the load transfers and the dissipation in the specified battery increases.

Figures 15 and 16 illustrate a serious problem in the analysis of space vehicles. The quantities of energy which flow in these vehicles are small, by the standards of conventional engineering. A typical Discoverer may ascend carrying primary batteries whose capacity is an average of approximately 300 w for the mission. This electrical load is determined from a power summary, which is simply the summation of the electrical requirements and duty cycles of all vehicle equipment. Unfortunately, it is a human trait to be conservative. Each equipment item is assigned an electrical

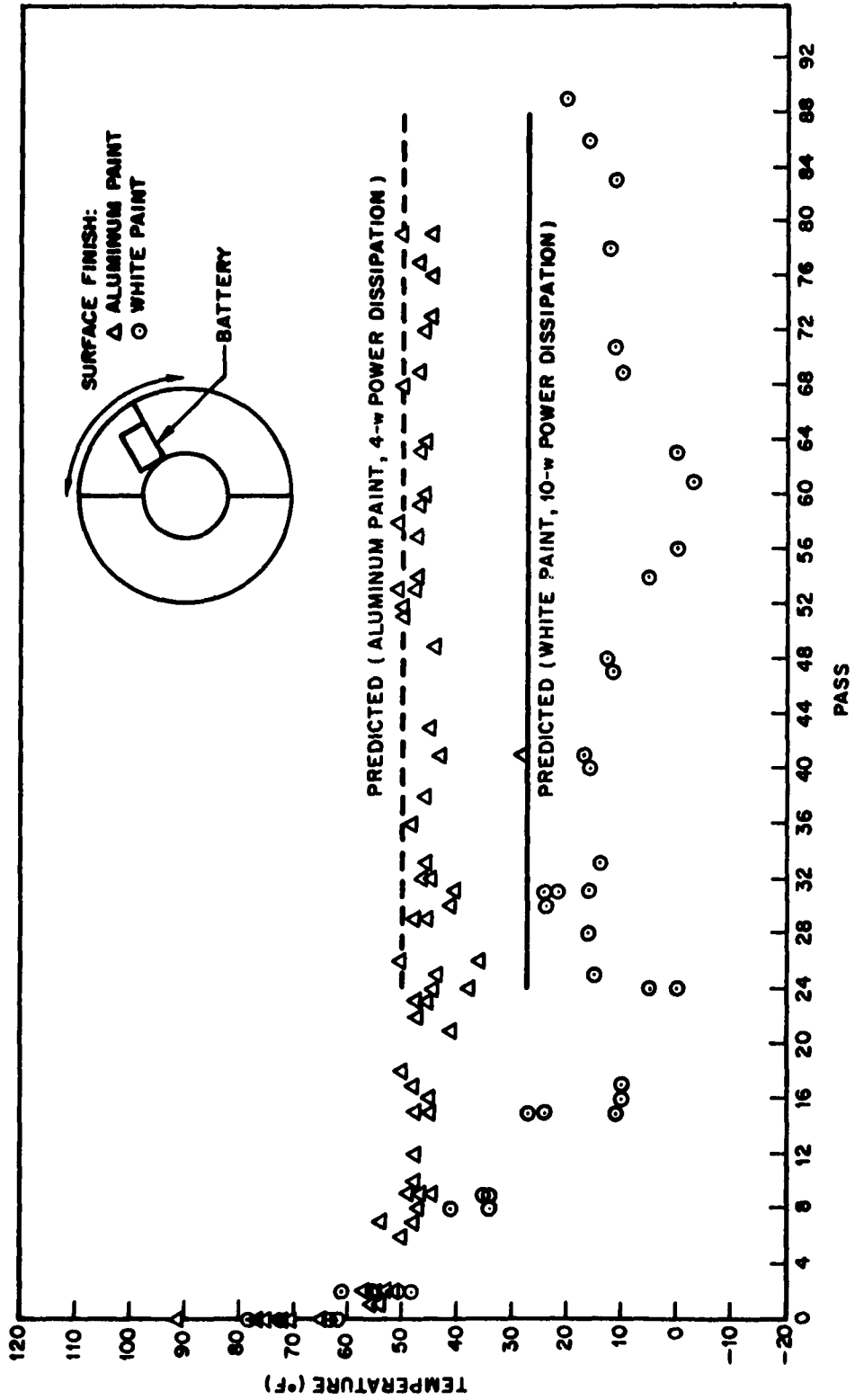


Fig. 13 Thermal Flight Data: Battery Case Temperature, 1

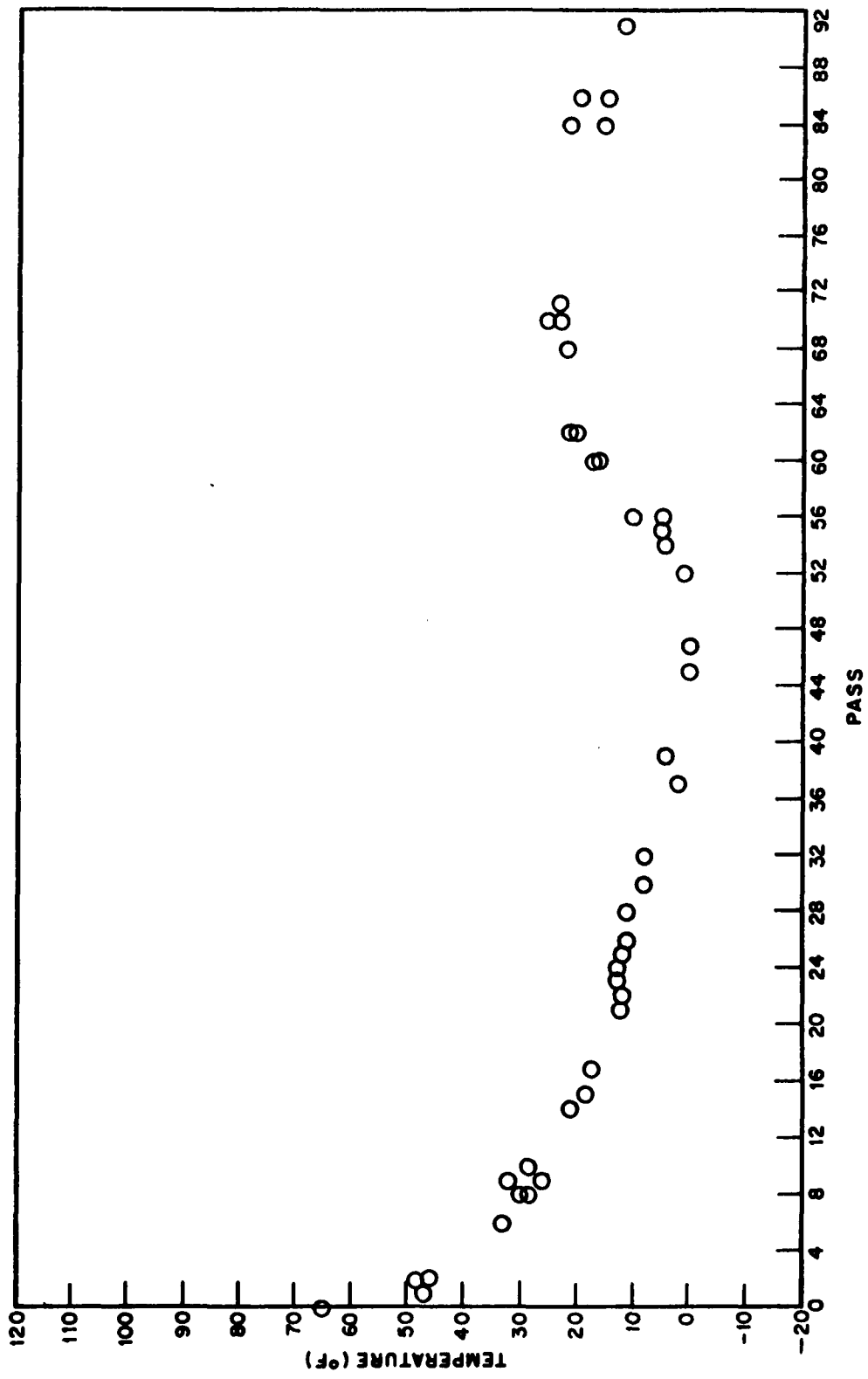


Fig. 14 Thermal Flight Data: Battery Case Temperature, 2

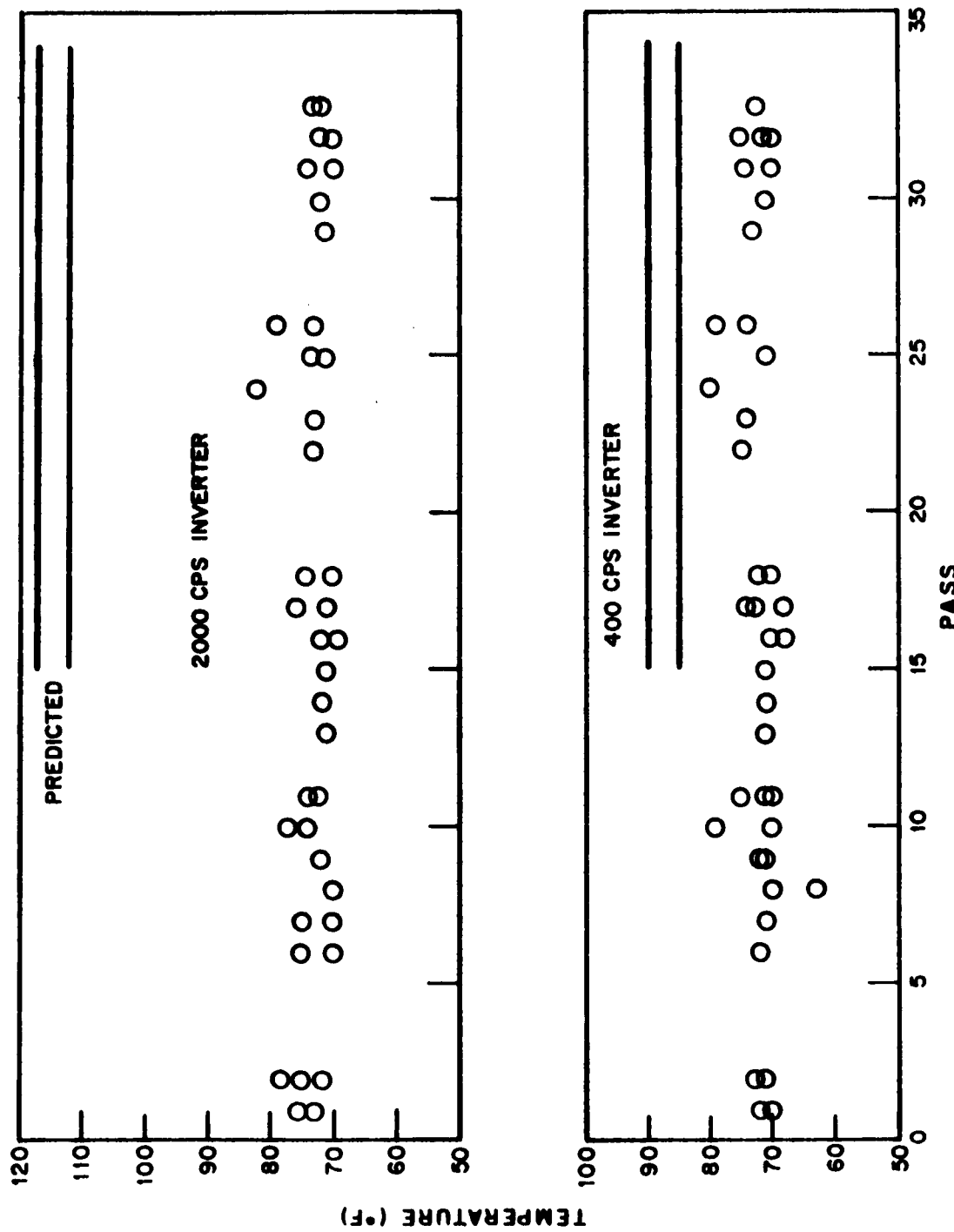
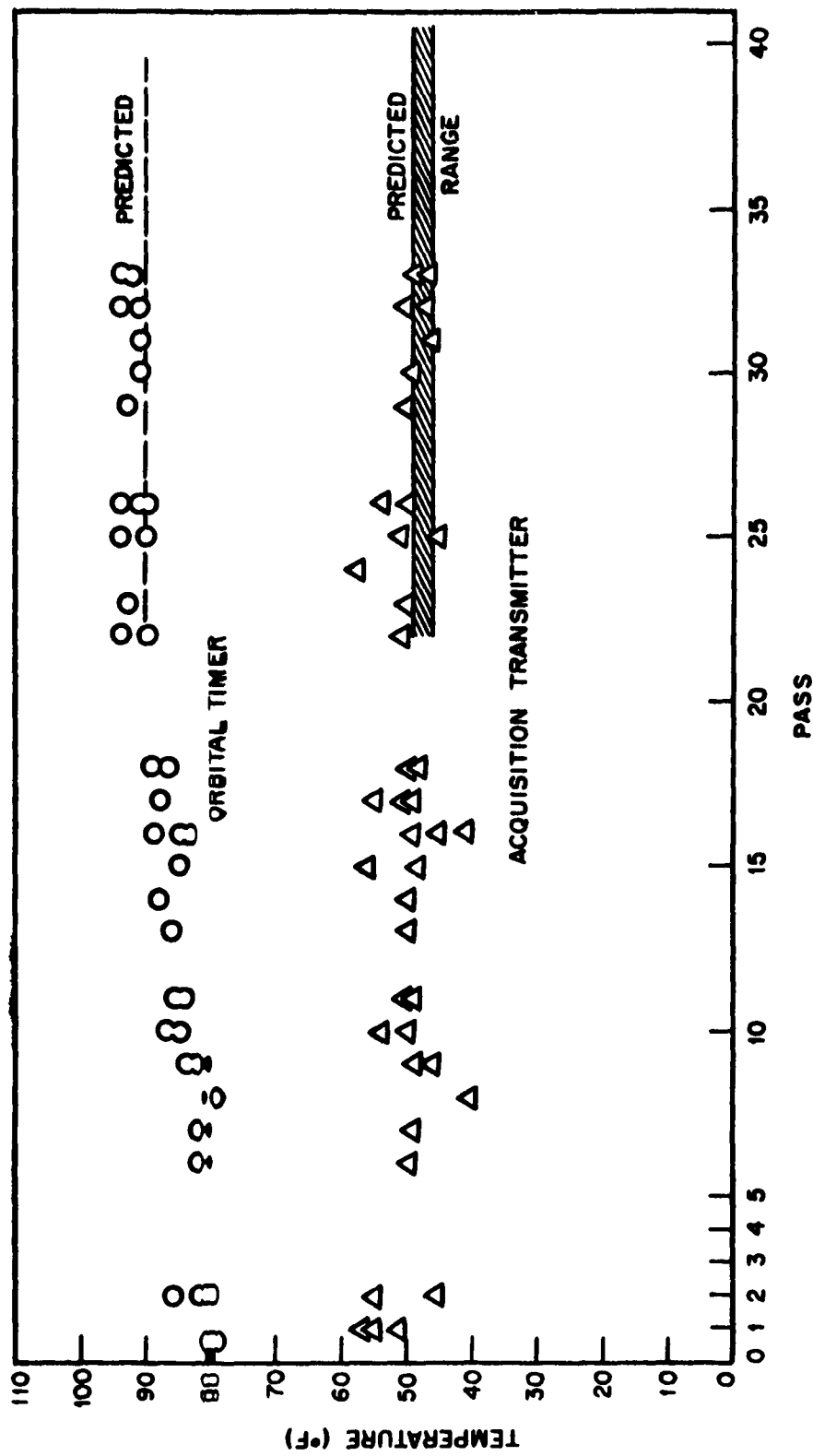


Fig. 15 Thermal Flight Data: Power Dissipation Predictions for Equipment Temperatures



input rating by its manufacturer or vendor when guaranteed performance is involved. To assure that no sample will ever fail to meet its specification, the electrical rating is chosen with sufficient conservatism. The extent of this conservatism is some inverse function of the vendor's knowledge of the performance of his equipment.

To maintain satisfactory temperature levels in equipment with small to moderate power dissipation ratings, the equipment mounting is designed to provide the desired thermal resistance to the spacecraft structure. The resistance is predicated on the equipment power dissipation and the predicted temperature extremes of the structure. It can be seen that conservatism in the electrical rating will result in a lower operating temperature for the equipment. The effects are more far-reaching, however - the adjacent structure will also be colder, and may thus affect other equipment in the vicinity. A final effect acts on the vehicle batteries. Battery internal dissipation, which appears as heat, is an exponential function of current drain. A cumulative conservative error in total vehicle power drain may then result in a serious effect on battery temperatures, which must be held between rather narrow limits for efficient operation.

Figure 15 presents data and predictions for two power inverters. In both cases the prediction is higher than data. It is assumed here, too, that the values supplied for internal dissipation are pessimistically high. The flight data show satisfactory temperatures; therefore, no further analysis was made. Figure 16 shows similar information for an orbital timer and an acquisition transmitter. The orbital timer is internally temperature controlled by a heater of known dissipation, while the transmitter dissipates a very small amount of energy continuously. Definitive knowledge of these devices facilitates the accurate predictions shown.

The effect on skin of orbit angle with respect to the sun is shown in Fig. 17 for orbits of 0 deg (noon launch) and 45 deg (3 o'clock). The temperatures shown are measured on an area receiving very little or no insolation at noon but appreciable amounts on a 3 o'clock launching. The wide band of predicted limits accounts for the swings as the vehicle alternately moves into and out of the sunlight; the limits form an envelope of maximums and minimums.

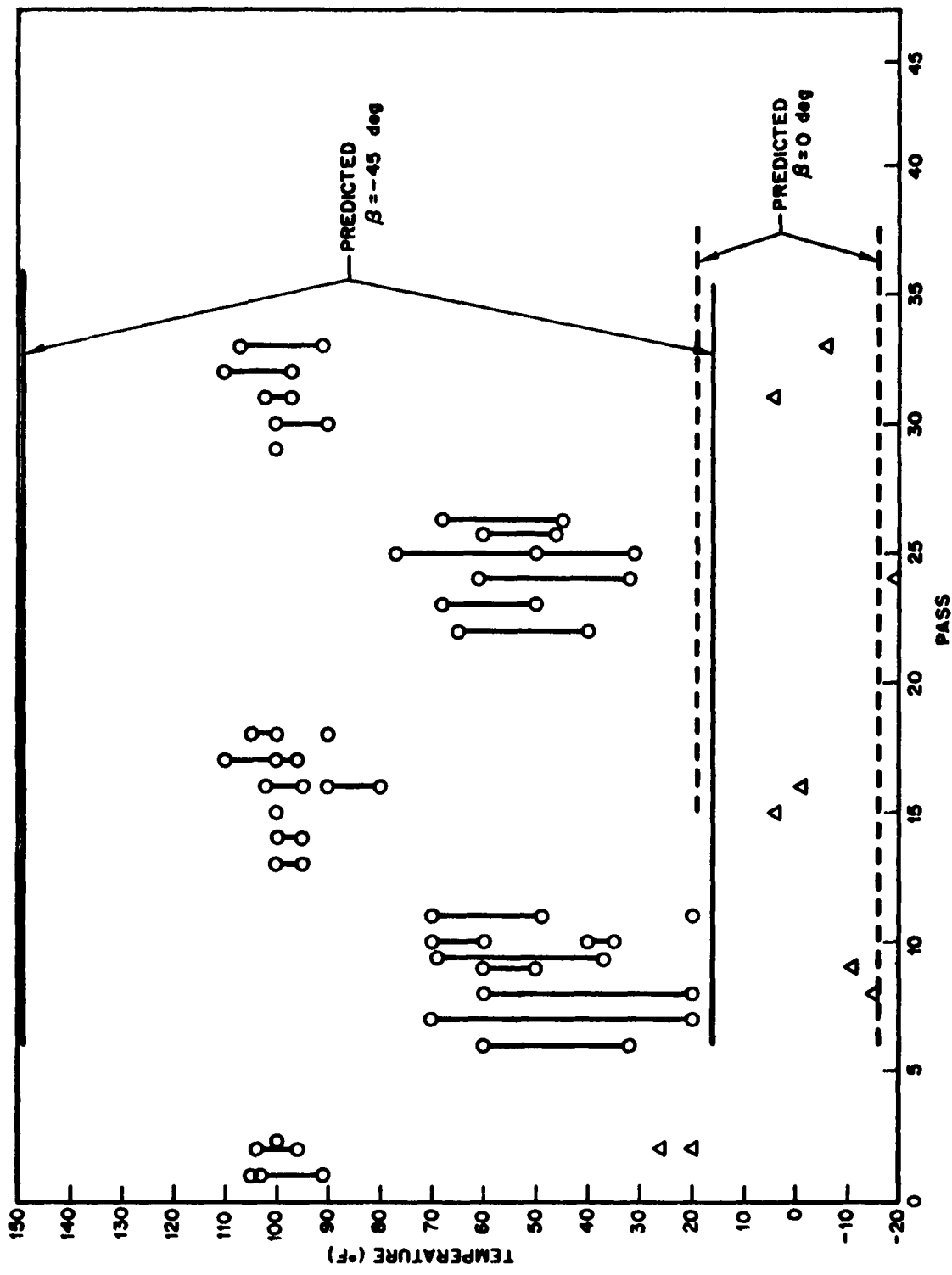


Fig. 17 Thermal Flight Data: Cylindrical Skin Temperature for Aluminum Paint

These swings are one of the fundamental problems in passive thermal control. Many vehicles must function through a large launch window, which, coupled with the alternate heating and cooling of each pass, imposes wide temperature extremes on the exterior skin and adjacent structure. It is probable that the limits of passive control are being reached; active systems will be called upon more frequently in the future.

A problem which became apparent only after the Discoverer had made many successful flights had its cause in the later afternoon launches.

This orbit results in shading of one cluster of the cold gas attitude control valves. The valves then display a sensitivity to low temperatures which results in hysteresis eventually leading to limit cycle oscillation and loss of control. Figure 18 shows predictions for the valve temperatures on both the cold and hot sides. To hold temperatures at or above 10° F, a small electric heater and a thermostat were mounted on each cluster. The results are shown. The duty cycle of the heater, about 50%, was predicted quite accurately by means of the network analogizing the valve area, and confirmed by telemetered information.

Improvement in vehicle design can also be achieved by relatively crude and simple testing techniques in the laboratory. For example, the inertial reference package, which must be maintained at an elevated internal temperature to provide the proper environment for its gyros, is equipped with a thermostatically controlled electric heater. The average power consumption of this heater has been approximately 30 w. Laboratory testing of the package was carried out to determine the relationship between internal and outer housing temperature. As a result, the equipment mounting was redesigned to provide high conductive resistance. The radiation resistance is controlled to provide the minimum power requirement possible, based on most conservative adjacent skin temperature predictions. This solution is expected to result in a nominal saving of 20 w continuously. That energy total represents a battery weight saving of 75 lb on a 5-day mission.

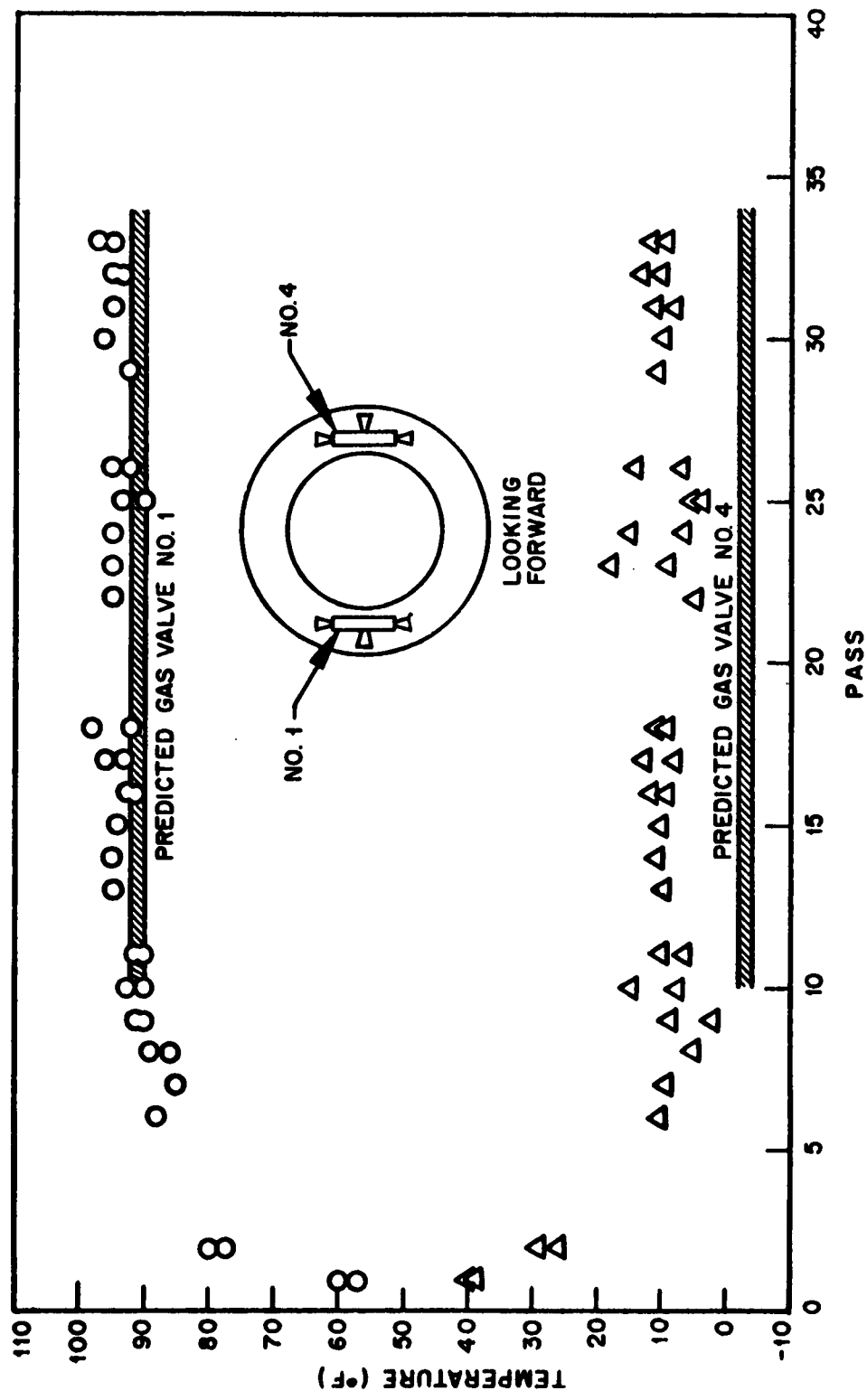


Fig. 18 Thermal Flight Data: Control Gas Valves

CONCLUDING REMARKS

The method in use, an electrical analogy solved by the finite difference technique, is capable of very acceptable performance in predicting space vehicle thermal performance. Improvement is necessary, however, in knowledge of equipment power dissipation. Vendors will always be conservative in furnishing this information, to guarantee the performance of their least efficient samples. This pessimism is not a conservative factor to the thermal analyst, because vehicle equipment has low-temperature as well as high-temperature limits.

It has been noted that contact resistance is not as large as originally had been expected. Much lower values are now used in analysis. In cases where equipment is mounted directly to flat structure, the contact resistance is assumed to be zero; the equipment and structural member area in contact are treated as a single node in the analysis. Radiation exchange within the vehicle is increasing in importance as analytical techniques become more sophisticated. A large primary battery in a thermally insulated mount may dissipate 1 w by conductive paths, but the radiation potential to an adjacent cold skin may amount to 5 w if the battery is at the desired temperature. If the battery total dissipation is less than 6 w, it will stabilize at a temperature satisfying the energy balance, a situation which may be unsatisfactory. Thus radiation barriers may be required.

Intelligent application of test results and analysis can conserve vehicle electrical energy. Testing may usefully involve complete vehicles or large vehicle sections in "space simulation" chambers, as well as other extremes of very simple laboratory work utilizing inexpensive facilities on individual equipment items.

The most significant improvement, however, will be acquisition of full orbit data. This is practical only by means of on-board tape recording with high-speed playback at the readout station. Analytical techniques will be improved only as much as they can be evaluated; lack of the temperature history over the full transient is a serious obstacle to evaluation.

REFERENCES

1. W. G. Comack and D. K. Edwards, "Effect of Surface Thermal Radiation Characteristics on the Temperature Control Problem in Satellites," Surface Effects on Spacecraft Materials, ed. F. J. Clauss, John Wiley & Sons, New York, 1960
2. D. K. Edwards, Computation of the Thermal Irradiation of Conical Satellites in Circular Orbits, TXA 30, Lockheed Missiles & Space Company, Sunnyvale, Calif., February 1959
3. R. Chesner, Incident Thermal Radiation on Horizontal and Vertical Cylinders and 15° Half-Angle Cones in Noon Circular Orbits, TXA 129, Lockheed Missiles & Space Company, Sunnyvale, Calif., 12 January 1960
4. R. E. Gaumer and L. A. McKeller, Thermal Radiative Control Surfaces for Spacecraft, LMSD-704014, Lockheed Missiles and Space Division, Sunnyvale, Calif., 1961

NOMENCLATURE

c_p	Specific heat, Btu/lb °F
C	Thermal capacity, Btu/°F
E	Earthshine (earth emissive power), 68.7 Btu/hr-ft ²
F	View factor
	Overall radiation interchange factor
k	Thermal conductivity, Btu/hr-ft °F
K	Thermal conductance, Btu/hr °F
m	Mass, lb
Q	Quantity of heat, Btu
q	Heat rate, Btu/sec
P_i	Internal power dissipation, Btu/sec
r	Thermal resistance, 1/k
R	Earth albedo, 16 Btu/hr-ft ²
S	Solar constant, 443 Btu/hr-ft ²
T	Temperature, °R
t	Time, sec
α	Absorptivity, dimensionless
β	Solar incidence angle
ϵ	Emissivity, dimensionless
σ	Stephan-Boltzmann constant 0.173×10^{-8} Btu/ft ² -hr(°R) ⁴
θ	Orbital position

Subscripts

a	Average
E	Earth emission
R	Albedo
S	Solar